

OPEN ACCESS

Comparison of transient and quasi-steady aeroelastic analysis of wind turbine blade in steady wind conditions

To cite this article: H Sargin and A Kayran 2014 *J. Phys.: Conf. Ser.* **524** 012051

View the [article online](#) for updates and enhancements.

Related content

- [Investigation of the effect of bending twisting coupling on the loads in wind turbines with superelement blade definition](#)
M O Gözcü and A Kayran
- [Model predictive control of a wind turbine modelled in Simpack](#)
U Jassmann, J Berroth, D Matzke et al.
- [Time-accurate aeroelastic simulations of a wind turbine in yaw and shear using a coupled CFD-CSD method](#)
D O Yu and O J Kwon



IOP | ebooks™

Bringing you innovative digital publishing with leading voices to create your essential collection of books in STEM research.

Start exploring the collection - download the first chapter of every title for free.

Comparison of transient and quasi-steady aeroelastic analysis of wind turbine blade in steady wind conditions

H. Sargin^{1,3} and A. Kayran²

¹Havelsan Inc. Mustafa Kemal Mahallesi, Çankaya, Ankara, Turkey

²Professor, METU Center for Wind Energy, METUWind,
Middle East Technical University, 06800, Ankara, Turkey

Abstract. In the preliminary design stage of wind turbine blade, faster and simpler methods are preferred to predict the aeroelastic response of the blades in order to get an idea about the appropriateness of the blade stiffness. Therefore, in the present study, applicability of the quasi-steady aeroelastic analysis of wind turbine blade is investigated in terms of how accurately the quasi-steady aeroelastic analysis predicts the deformed state of the blade at certain azimuthal positions. For this purpose, comparative study of transient and quasi-steady aeroelastic analysis of a composite wind turbine blade in steady wind conditions is conducted. To perform the transient analysis, a multi-body wind turbine model is generated with almost rigid components except for the dynamic superelement blade that is inverse designed. Transient analysis of the multi body wind turbine system is performed by imposing constant rotational speed to the main shaft and bypassing the controller. Quasi-steady aeroelastic analysis of the same composite wind turbine blade is performed, by coupling a structural finite element solver with a blade element momentum tool, in steady wind conditions at different azimuthal positions including the effect of the centrifugal and gravitational forces. Results show that for the wind turbine system taken as the case study, reasonably good agreement is obtained between the tip deflections and flapwise root shear forces determined by the transient aeroelastic analysis of the wind turbine and quasi-steady aeroelastic analysis of the blade only.

1. Introduction

In the design of wind turbine blades, for accurate load analysis, complete turbine model has to be generated in a multi-body framework, and transient aeroelastic analysis of the wind turbine system, which includes major components such as turbine blades, rotor hub and rotor shaft, gearbox, generator and tower, has to be performed. However, building the multi-body model of the complete wind turbine requires specialized software and detailed information about the major components which build-up the turbine system. In the preliminary design stage, faster and simpler methods are usually preferred to predict the aeroelastic response of the blades in order to get an idea about the appropriateness of the blade stiffness. For this purpose, quasi-steady aeroelastic analysis is an approach that is commonly employed in the preliminary design stage of wind turbine systems. In the early studies, external loads on wind turbines were evaluated by utilizing quasi-static aerodynamic calculations, with the effect of structural dynamics either ignored or included through the use of estimated dynamic magnification factors [1]. From the beginning of 1980s, more reliable methods of dynamic analysis of wind turbine systems were considered. Garrad presented a review work on the development of wind turbine

³ To whom any correspondence should be addressed.



modelling techniques [2]. Pedersen has performed a study focusing on the aeroelastic codes for wind turbine calculations [3]. A more recent study on the comprehensive review of wind turbine aeroelasticity is performed by Hansen et al. [4]. The number of studies focusing on the wind turbine aeroelasticity in the literature can be increased. In general, there are two major ways of performing dynamic analysis of wind turbine systems. One approach is to have detailed finite element models of the sub-structures of the wind turbine system in the multi-body model of the wind turbine. Finite element models of the sub-structures can be either detailed 3D finite element models or 1D finite element models representing the slender sub-structures such as blades, tower etc. However, due to the complexity of the wind turbine system, including detailed 3D finite element models of the sub-structures into the multi-body model of the wind turbine system is not preferred due to the modelling effort needed and the computational cost of transient aeroelastic analysis of the wind turbine system. Therefore, current trend is to use geometrically linear and non-linear beams models of the tower and the blades in the multi-body model of the wind turbine system. In such models, drive train components are modelled by multi-body simulation features, such as springs, kinematic joints etc., inside real finite elements models. Another reduced order modelling approach is to use superelement models of the sub-structures of the wind turbine system in the multi-body model. In the superelement modelling approach, large displacements and rotations in space are allowed, with the only limitation that with respect to the local frame fixed to the sub-structure, sub-structure behaves geometrically linear. Blades, tower, gearbox, bedplate are typical sub-structures that are modelled as superelements in the wind turbine system. With superelement restitution, displacements, forces and stresses within a superelement can be retrieved on the basis of a given transient analysis.

In the present article, a preliminary study is performed on the comparison transient and quasi-steady aeroelastic analysis of a composite wind turbine blade in steady wind conditions. Comparison of the blade tip displacements obtained by the quasi-steady aeroelastic analysis of the blade only and blade tip displacements obtained by the transient aeroelastic analysis of the wind turbine system are made at different azimuthal positions. The applicability of quasi-steady aeroelastic analysis is investigated in terms of how accurately the quasi-steady aeroelastic analysis predicts the deformed state of the blade at certain azimuthal positions for the turbine taken as the case study. Reasonably good agreement is seen between the tip deflections obtained by the transient aeroelastic analysis of the complete wind turbine system and quasi-steady aeroelastic analyses of the blade only. It is considered that for the wind turbine system taken as the case study, quasi-steady aeroelastic analysis can be reliably used for the preliminary design study of the wind turbine blade.

2. Inverse design of the reference blade

In the present study, unsteady aerodynamics experiment (UAE) research wind turbine NREL Phase VI is chosen as the reference turbine model [5] to perform the inverse design of the turbine blade for the purposes of conducting quasi-steady aeroelastic analysis of the blade and transient aeroelastic analysis of the wind turbine system. The root of the reference blade starts at the blade-hub connection at a radius of 0.508 m from the center of the hub. Between the radial locations 0.508 m - 0.660 m, blade has a circular cross-section. Transition part of the blade lies between 0.660 m and 1.257 m. From the end of the transition section to the tip of the blade, the blade has NREL S809 airfoil shape with linear taper and nonlinear twist distribution. It should be noted that although sectional beam properties of blade used in the (UAE) research wind turbine NREL Phase VI exist [6], laminate definitions in the spanwise and chordwise directions could not be determined from the literature. In order to account for the coupling stiffness effects due to material lay-out and blade geometry appropriately, in the present study 3D blade geometry is used in the quasi-aeroelastic analysis of the blade, and superelement of the blade is used in the transient aeroelastic analysis of the wind turbine system. Therefore, inverse design of the three dimensional blade is performed such that sectional flapwise stiffness and mass properties of the 3D blade approximately match the corresponding properties of blade of the unsteady aerodynamics experiment (UAE) research wind turbine [6]. Matching of the blade mass density is accomplished by assigning appropriate mass densities to the material in each blade section so that

sectional blade mass densities approximately match the sectional blade mass densities of the NREL blade. Although the assigned mass densities in each section do not reflect the actual density of the material used in the inverse design, sectional mass properties of the inverse designed blade match the mass properties of the NREL blade within %10. It should be noted that the goal of the inverse design methodology is to come up with a blade design, with realistic stiffness and mass properties, to be used in the quasi-steady aeroelastic analysis of the blade and transient aeroelastic analysis of the wind turbine system. Therefore, exact match of the sectional beam properties of the inverse design blade with the sectional beam properties of the NREL blade is not required. The following materials are used in the D-Spar cap and trailing edge of the wind turbine blade to match the flapwise stiffness and sectional mass of the blade with the corresponding properties given for the NREL Phase VI blade.

- Prepreg hybrid Carbon Fiber AS4 12k/997 Unidirectional / fiberglass Triax, 70% 0° for the D-Spar cap [7]
- E-Glass 7781/EA 9396 8-harness satin weave fabric for rear part of the wing [7]

For each section of the blade, appropriate laminate definitions are made for the D-spar cap and trailing edge regions. Two dimensional finite element of each blade section is then prepared in PreVABS [8] whose output is processed by the variational asymptotic beam section code VABS [9] to calculate the sectional beam properties of the blade which are in turn compared with the known beam properties of the NREL blade [6]. Iterations continue until acceptable differences between the sectional beam properties are obtained for each section of the blade. Figure 1 compares the sectional flapwise bending stiffness of the inverse designed blade and the NREL blade [6], respectively. It is seen that very good match of the flapwise stiffness has been obtained with the implementation of the inverse design approach.

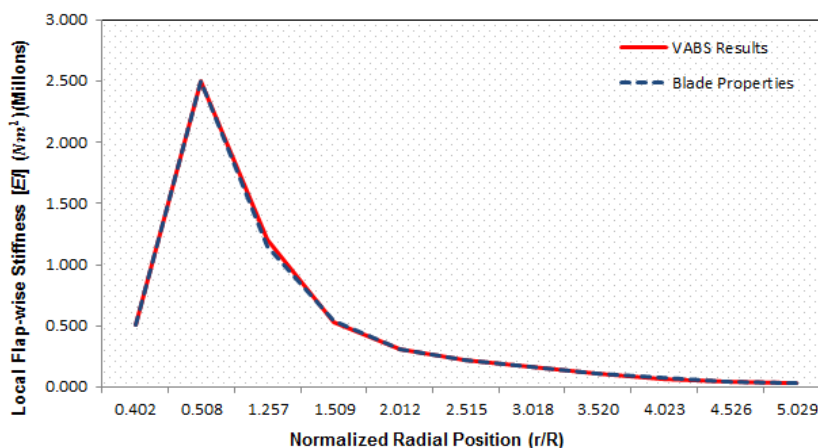


Figure 1. Comparison of the variation of the flapwise stiffness of the NREL blade [6] and the inverse design blade

3. Quasi-steady aeroelastic analysis of the wind turbine blade

Quasi-steady aeroelastic analysis of the blade is performed by coupling the blade element momentum solver of the wind turbine performance predictor tool, WT_Perf [10] with the finite element solver MSC Nastran. Aerodynamic coefficients obtained by WT_Perf are used to calculate the sectional lift, drag and moment forces at the aerodynamic center of each blade section. Aerodynamic forces calculated at the aerodynamic center of each blade section are applied to the nodes created at the aerodynamic center locations in the structural finite element model. In addition, gravity and centrifugal forces due to the rotation of the wind turbine blade are created by generating inertia load cards, and assigning the gravitational acceleration and the rotation speed to the whole 3D blade as body forces accordingly. For the 0°, 90° and 180° azimuthal locations, the direction of the gravity vector is changed accordingly to take the gravity forces into account correctly. The interaction of the

aerodynamic model and the structural finite element model is performed in a loosely coupled fashion. At each iteration, after the blade deformation is determined, incremental changes in the angle of attack values at each blade section are calculated. Incremental changes in sectional angle of attack values in turn cause incremental changes in the aerodynamic loading which are then applied to the structural finite element model to calculate the next set of incremental changes in angle of attack values at the blade sections. The iterative process is repeated until the blade deformation converges within a prescribed tolerance. Aerodynamic forces acting at the aerodynamic center of blade sections are distributed to the suction side nodes of the finite element model by means of multi-point constraint element RBE3 that is available in MSC Nastran [11]. RBE3 element defines a constraint relation in which the motion at a reference grid point is the least square weighted average of the motions at other grid points [11]. Forces and moments applied to reference points are distributed to a set of independent degrees of freedom based on the RBE3 geometry and local weight factors. The manner in which the forces are distributed is analogous to the classical bolt pattern analysis. The force and moment is transferred directly to the weighted center of gravity location along with the moment produced by the force offset. The force is distributed to the bolts proportional to the weighting factors. The moment is distributed as forces, which are proportional to their distance from the center of gravity times their weighting factors. For the distribution of the forces applied at the aerodynamic center, weight factors are taken as 1 since nodes represent same size bolts. Figure 2 shows the variation of the flapwise and leadwise forces at the blade sections for the 90° azimuth. Flapwise and leadwise forces are calculated by decomposing the lift and the drag forces calculated by WT_Perf with respect to the blade root reference system. Figure 3 shows the distribution of aerodynamic forces applied at the aerodynamic center of each blade section to suction side nodes by RBE3 elements.

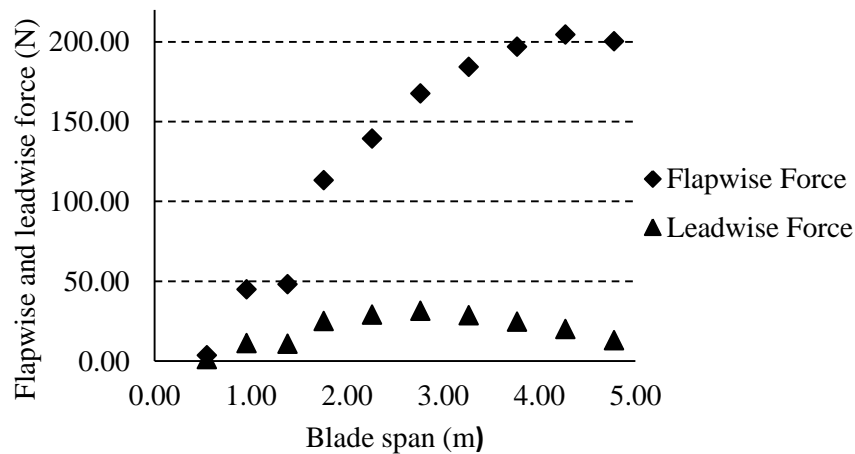


Figure 2. Variation of sectional flapwise and leadwise forces along the blade span

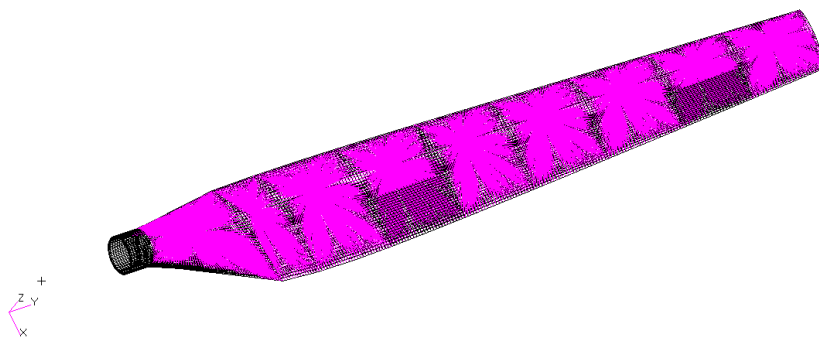


Figure 3. Distribution of aerodynamic forces to suction side nodes

It should be noted that as it is seen in Figure 2, in accordance with the blade element momentum theory, aerodynamic forces calculated by WT_Perf at the aerodynamic center of each blade element are distributed to the nodes on the suction side of the corresponding blade element only. In the quasi-steady aeroelastic analysis, the cylindrical root part of the blade ($r=0.508$ m- 0.66 m), shown in Figure 2, is clamped. It is considered that in the actual assembly of the blade to the rotor hub, the cylindrical root of the blade is fixed to the rotor hub which is assumed to be rigid in the quasi-steady aeroelastic analysis. Quasi-steady aeroelastic analysis of the blade is performed at 15 m/s steady wind speed with a wind shear exponent of 0.2 . As shown in Figure 4, calculations are performed at azimuthal locations of 0° , 90° and 180° .

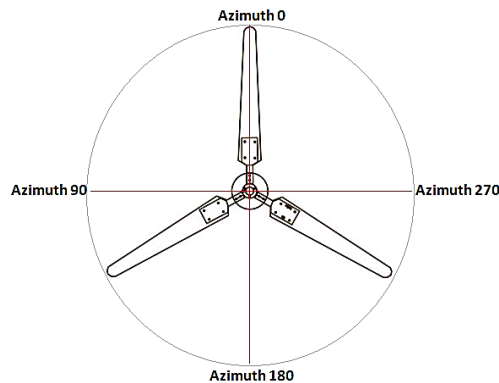


Figure 4. Azimuthal locations where quasi-steady aeroelastic analyses are performed

During the quasi-aeroelastic analysis process, incremental changes in the aerodynamic loads are computed by utilizing the “shifting nodes” feature of MSC.Patran. Figure 5 shows that at each iteration, all node locations are shifted to the deformed positions. After the shifting of the nodes, new positions of the node locations at the leading and trailing edges of each blade section are recorded, and incremental changes in the sectional angle of attack values are calculated at each blade element. As an example, for azimuth 90° , Table 1 gives the incremental changes in angle of attack values with the iteration number at each blade element. The first blade element corresponds to the circular root where there is no lift. It is seen that in three iterations, incremental changes in the angle of attack values become almost negligible. Therefore, in the quasi-steady aeroelastic analysis, four iterations are performed. The fourth iteration essentially gives the same deformation of the blade as the third.

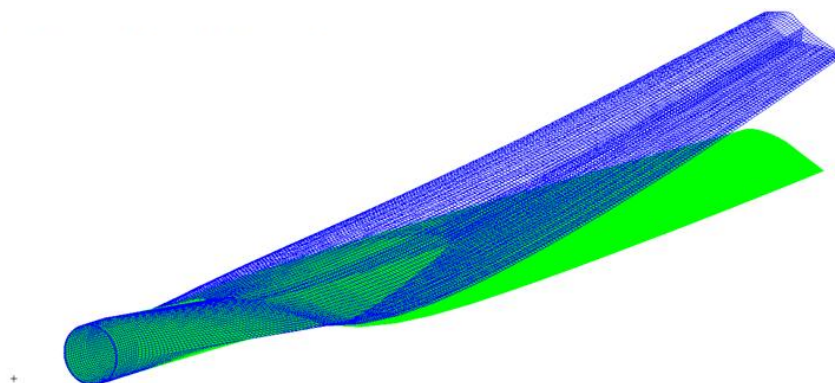


Figure 5. Shifting of nodes to the deformed positions

Table 1. Incremental changes in angle of attack values with the iteration number - Azimuth 90°

Blade element	1 st iteration (Deg.)	2 nd iteration (Deg.)	3 rd iteration (Deg.)
2	-0.0346	-0.00014	-0.00006
3	-0.2696	-0.00197	-0.00023
4	-0.3287	-0.00249	-0.00027
5	-0.3908	-0.00296	-0.00032
6	-0.4017	-0.00316	-0.00033
7	-0.4117	0.00331	-0.00034
8	-0.4024	0.00330	-0.00034
9	-0.4348	0.00362	-0.00037
10	-0.4102	0.00310	-0.00034

Table 2 gives the maximum axial tip displacements towards downwind obtained as a result of quasi-aeroelastic analysis of the blade at three different azimuthal locations. It is seen that the change in the maximum tip displacement in each iteration is very small. This is an indication that the inverse designed blade structure is actually very rigid. However, the whole process of quasi-steady aeroelastic analysis would not change if the blade structure were more flexible. For flexible blade structures, quasi-steady aeroelastic analysis could still be performed if geometrically non-linear solver MSC Nastran (Sol 106) is used as the structural solver instead of the linear solver Sol 101. However, for long and flexible blades, one would likely to have larger differences between the results of quasi-aeroelastic analysis and transient aeroelastic analysis because of the differences in the nature of transient aerodynamic loading on a stiff blade and on a highly flexible and slender blade.

Table 2. Maximum axial tip displacements towards downwind at different azimuthal positions

# of Iterations	Tip Displacement Azimuth 0° (mm)	Tip Displacement Azimuth 90° (mm)	Tip Displacement Azimuth 180° (mm)
1 st Iteration	110.5	102.5	99.6
2 nd Iteration	111.6	103.2	99.8
3 rd Iteration	111.7	103.3	100
4 th Iteration	111.7	103.3	100

4. Multi-body modeling of the wind turbine and transient aeroelastic analysis of the blade

In the design of wind turbine blades, for accurate load analysis, complete turbine model has to be built in a multi-body framework and transient aeroelastic analysis of the wind turbine system which includes major components such as turbine blades, rotor hub and rotor shaft, gearbox, generator and tower has to be performed. Building the multi-body model of the complete wind turbine requires specialized software and detailed information about the major components which build-up the turbine system. For this purpose, in the present study, multi-body dynamic code Samcef Wind Turbines (SWT) is utilized for performing the transient aeroelastic analysis of the blade [12]. Samcef Wind Turbines integrates the aerodynamic, structural and control features of the wind turbine in a fully dynamic environment. Aerodynamic solver of SWT is based on BEM theory with typical corrections such as tip and hub losses, tower shadow, and deactivation of induction factors at low tip speed ratios. Samcef Wind Turbines also has built-in semi-empirical sub-models to treat unsteady aerodynamics with higher accuracy. Specifically, SWT has dynamic wake sub-model, skewed flow correction sub-model and dynamic stall sub-models which are of Beddoes-Leishman type. The controller is integrated to the wind turbine model by means of dynamic link library which can be used for typical wind turbine simulations. Multi-body simulation of the wind turbine system is performed by the implicit non-linear finite element solver Samcef Mecano [13] which has the ability to allow the use of multi-body simulation features, such as kinematic joints etc., inside real finite elements models. Transient

simulations are performed in time domain taking into account the structural, multi-body, aerodynamic and control features in a fully non-linear dynamic way with strong coupling.

In the present study, to conduct the multi-body dynamic analysis of the wind turbine system, dynamic superelement of the turbine blade is created in the Samcef Field [14] and it is introduced into the multi-body model of the wind turbine system. Before the generation of the dynamic superelement of the blade, three dimensional finite element model of the blade is created in Samcef Field in a similar manner to the creation of the finite element model in MSC Patran that is described before. In order to reflect the stiffness and mass properties of the blade appropriately, three dimensional finite element model of the blade is used rather than the beam model. It should be noted that neither MSC Nastran nor SWT have beam formulations that are suitable for modelling composite blades with coupling coefficients. Therefore, in the quasi-steady aeroelastic analysis performed by MSC Nastran, three dimensional shell finite element model of the blade is used. On the other hand, in the transient aeroelastic analysis performed by SWT, dynamic superelement of the blade is used since SWT does not allow the use of three dimensional finite element model in the multi-body model of the wind turbine system. Figure 6 shows the generation of the superelement of the wind turbine blade. In the superelement generation process, at each blade section a retained node must be created at the %25 chord of the blade measured from the leading edge of the blade. Once the superelement of the blade is imported into the multi-body model of the wind turbine system, retained nodes are used for applying external loads on the turbine blade. Retained nodes are also used as the connector nodes of the blade to the wind turbine system through the rotor hub. Therefore, at the root section retained node is created at the center of the circular cross-section. As shown in Figure 6, retained nodes are tied to the faces on the leading and trailing edge of the blade. In the current study, the link between the retained nodes and the faces of the related blade section is established via mean elements which connect the retained node, which is taken as the slave node, to the master nodes on the faces of the particular section. By the use of mean elements, mean displacement of the master nodes is assigned to the retained node. It should be noted that superelement could also be generated by the use of rigid elements between the master and the slave nodes. Such superelements behave more rigid than the real structure, on the other hand, superelement generated by mean elements is more flexible than the real structure since no additional rigidity is added. Therefore, the real behaviour would be between these two idealizations. A critical step in the generation of the superelement of the wind turbine blade is to assign the correct displacement boundary conditions to the retained node at the root of the blade that connects the blade to the rotor hub in the wind turbine system. At this node, a free rotation about the pitch axis must be defined to allow for the pitch motion of the blade in the multi-body simulation of the wind turbine system. It should be noted that as shown in Figure 6, the cylindrical root of the blade is connected to the blade-hub link node on the very stiff rotor hub node via mean elements established between the retained node at the blade root and the cylindrical root of the blade.

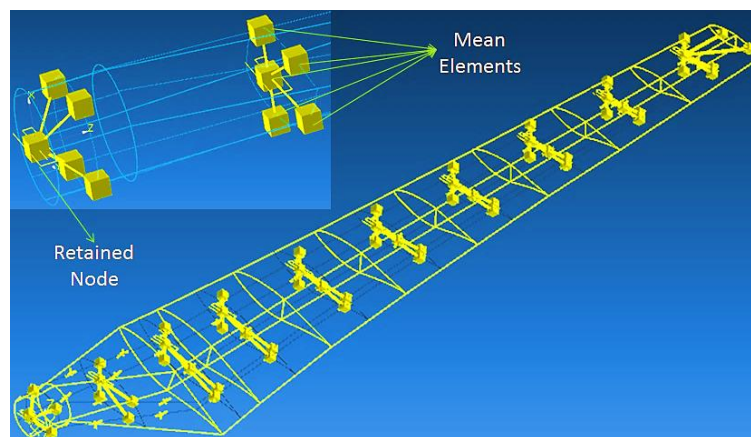


Figure 6. Generation of the superelement of the wind turbine blade

Verification of the superelement of the blade is done in Samcef by performing modal analysis of the baseline blade which is clamped at the root. Free vibration frequencies of the first five modes in the still air obtained by the complete three dimensional finite element model of the blade are compared with the frequencies obtained by the modal analysis of the superelement of the blade in Table 3.

Table 3. Comparison of first five frequencies of the turbine blade clamped at the root

Modes	3D FE Model (Hz)	Superelement Blade (Hz)
1	4.13	4.13
2	8.32	8.33
3	17.52	17.54
4	28.40	28.44
5	32.47	32.52

As it is seen from Table 3, very good agreement exists between the natural frequencies obtained by the 3D finite element model and superelement of the blade. Such an agreement is an indication that the superelement of the blade represents the stiffness and mass properties of the three dimensional blade accurately, and it can be included in the multi-body model of the complete wind turbine system.

To study the aeroelastic response of the superelement blade, a 20 kW multi-body wind turbine model is created in SWT. For realistic and reliable computation of the internal loads in the wind turbine system, several sub-structures, including the controller, are included in the multi-body model of the turbine. For the parameters of the wind turbine, known properties of NREL Phase VI turbine are taken as the reference and aerodynamic coefficients of the NREL S809 airfoil obtained from the wind tunnel tests [5] are used in the transient aeroelastic analysis. For the drive train model, the so-called FAST drive train model that is available in SWT is included in the wind turbine multi-body dynamic model. Figure 7 shows the wind turbine model with the FAST drive train. For explanation purposes, typical sub-components that exist in FAST drive train are also shown in Figure 7. FAST drive train includes the bedplate, simple gearbox and generator, rotor shaft, coupling shaft, nacelle, main frame and rear frame. When FAST drive train is used, it is not necessary to include components of the drive train separately into the multi-body model of the wind turbine system. In case of separate inclusion of the drive train components, detailed properties must be provided for each component. Therefore, in the present study, to keep the modeling effort of the wind turbine system simple, FAST drive train is used. The default properties of the FAST drive train are initially replaced by the known properties of the NREL Phase VI turbine [5,6].

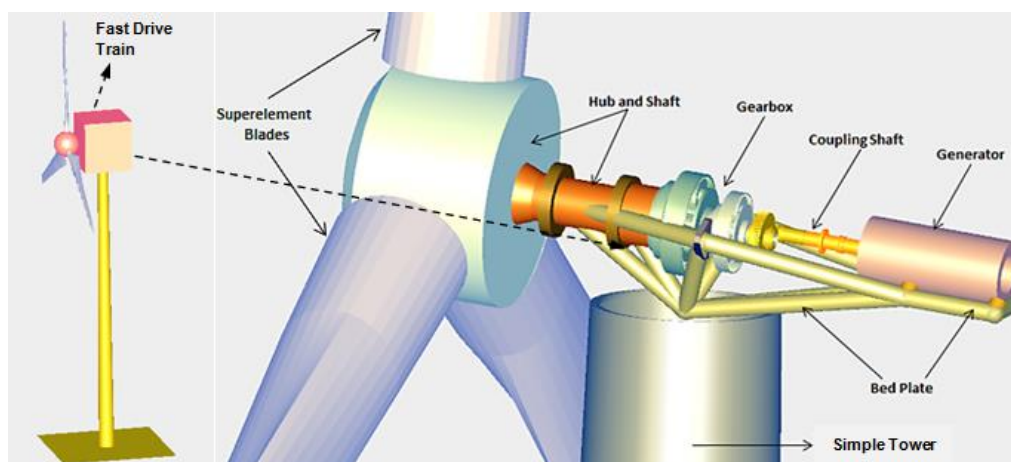


Figure 7. Multi-body model of the wind turbine system with the FAST drive train

In order to include only the transient effects due to the rotation of the wind turbine blades in the multi-body simulation of the wind turbine system, multi-body model of the wind turbine is created

with almost rigid drive train and tower as the main sub-structures. By assigning a modulus of elasticity of 1000 times the modulus of elasticity of steel to the tower, flexibility of the tower is eliminated. Similarly, equivalent drive shaft torsional spring constant value is also increased 1000 times compared to the default value given for the FAST drive train in SWT. By eliminating the flexibility of the drive train and the tower, more realistic comparison of the results of the transient aeroelastic analysis of the complete wind turbine system with the results of the quasi-steady aeroelastic analysis of the turbine blade can be made. In order to compare the results of the quasi-steady aeroelastic analysis with the results of the transient aeroelastic analysis, wind turbine is rotated at constant speed of 72 rpm. For this purpose, constant rotational speed is applied to the control node at the main shaft main bearing which is the closest bearing to the rotor hub shown in Fig. 7. In addition, rotor conicity and tilt angle is not considered and pitch angle of the blades is fixed at 0 degree. As for the aerodynamics, except for the tip losses, which are also taken into account in the WT_Perf calculations, not other unsteady effects are considered in the transient aeroelastic analysis. Figure 8 gives the axial displacement towards downwind of the blade tip section for 30 seconds of rotation of the wind turbine blade at constant rotational speed. It is seen that due to the wind shear, displacement fluctuates within a band.

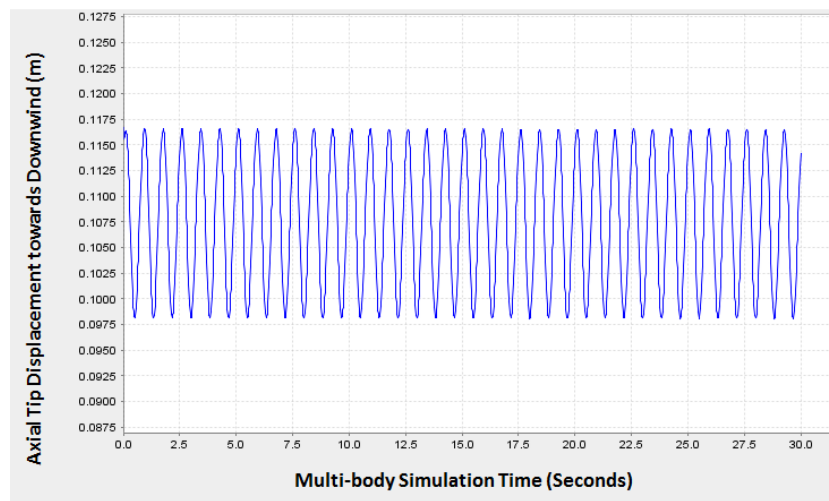


Figure 8. Axial tip displacement of the blade towards downwind

Comparison of the blade tip axial displacements towards downwind obtained by the quasi-steady aeroelastic analysis of the blade only and transient aeroelastic analysis of the wind turbine system is given in Table 4 for different azimuthal positions. For the blade and the wind turbine system studied, reasonably good agreement is observed between the tip displacements at different azimuthal positions. It is noted that in the transient analysis, tip deflections towards downwind are not equal to each other for the 90° and the 270° azimuthal positions. The reason for the difference is due to the wind shear effect. In the 0° azimuthal position, the blade is vertically up, therefore aerodynamic forces are high, and as the blade rotates to the 90° azimuthal position, due to the transient effect of the higher aerodynamic forces, the blade deflection at the 90° azimuthal position is higher than the blade deflection at the 270° azimuthal position. On the other hand, blade comes to the 270° azimuthal position from the vertically down position of the blade at the 180° azimuthal position where the aerodynamic forces are lowest due to the wind shear effect. Obviously, quasi-steady aeroelastic analysis predicts the same displacements at the 90° and the 270° azimuthal positions of the blade. The pronounced difference in the tip displacement at 90° azimuth is attributed to the transient effect associated with the rotation of the blade. In the transient analysis, it is seen that the peak tip displacement does not occur at 0° azimuth but it occurs at about 47.5° azimuth.

Table 4. Comparison of blade tip axial displacements towards downwind

Azimuth	Quasi-steady aeroelastic analysis (mm)	Transient aeroelastic analysis (mm)
0°	111.7	114
90°	103.3	113.8
180°	100	99.9
270°	103.3	101.9

Table 5. Comparison of flapwise shear force at the blade root for different azimuthal positions

Azimuth	Quasi-steady aeroelastic analysis (N)	Transient aeroelastic analysis (N)
0°	1364.3	1379.1
90°	1298	1312.2
180°	1238.2	1204.6
270°	1298	1293

Table 5 compares the flapwise shear forces at the blade root predicted by the quasi-steady aeroelastic analysis of the blade and transient aeroelastic analysis of the wind turbine system. Since the flapwise shear force is mainly due to aerodynamic loading, the good agreement of the shear forces obtained by the quasi-steady aeroelastic analysis of the blade and transient aeroelastic analysis of the wind turbine system is an indication that transient effects due to the rotation of the blade is not significant on the aerodynamic loading on the blade for the wind turbine system studied.

5. Conclusion

Comparative study of quasi-steady and transient aeroelastic analysis of a composite wind turbine blade in steady wind conditions is conducted. Quasi-steady aeroelastic analysis of the blade showed that inverse designed NREL Phase VI blade structure is actually very rigid. Results also show that for the NREL Phase VI wind turbine system considered in the case study, reasonably good agreement is obtained between the tip deflections and the flapwise root shear forces obtained by the transient aeroelastic analysis of the complete wind turbine system and the quasi-steady aeroelastic analysis of the blade only for the steady wind load case. For the NREL Phase VI wind turbine system considered in the case study, it is concluded that in the preliminary design stage, quasi-steady aeroelastic analysis of the blade can be used reliably in predicting the overall deformation of the blade and sectional blade forces which would otherwise be obtained by the multi-body simulation of the complete wind turbine system. Finally, it should be noted that the present study is performed in steady wind conditions. Quasi-steady aeroelastic analysis can be used in the preliminary design for the initial sizing of the internal blade structure. However, in the detailed design phase, multi-body simulations of the wind turbine system must be performed considering all load cases to fine tune the initial sizing obtained utilizing quasi-aeroelastic analysis.

Acknowledgments

This work was supported by the Metu Center for Wind Energy and Scientific and Technological Research Council of Turkey (TÜBİTAK), Project No: 213M611.

References

- [1] Quarton D C, The Evolution of Wind Turbine Design Analysis-A Twenty Year Progress Review 1998 *Wind Energy* **1**(3) 5
- [2] Garrad A D, Dynamics of Wind Turbines 1983 *IEE Proc.* **130** 523
- [3] Pedersen B M, State of the Art of Aeroelastic Codes for Wind Turbine Calculations 1996 *Proc. 28th Meet. Experts, IEA Annex XI* 1
- [4] Hansen M O L, Sorensen J N, Voutsinas S, Sorensen N, Madsen H Aa, State of the Art in Wind Turbine Aerodynamics and Aeroelasticity 2006 *Progress in Aerospace Sciences* **42** 285
- [5] Hand M M, Simms D A, Fingersh L J, Jager D W, Cotrell J R, Schreck S J, Larwood S M, Unsteady Aerodynamics Experiment Phase VI: Wind Tunnel Test Configurations Available

- Data Campaigns 2001 NREL/TP-500-29955, Golden, CO, NREL
- [6] J.M. Jonkman J M, Modeling of the UAE Wind Turbine for Refinement of FAST-AD, NREL/TP-500-34755, Golden, CO, National Renewable Energy Laboratory 2003
- [7] Composite Materials Handbook, Polymer Matrix Composites Material Properties, MIL-HDBK17-2F 2002 **2**
- [8] Chen H, Yu W, Manual of PreVABS, December 2008,
<http://analyswift.com/wp-content/uploads/2012/10/PreVABS-Manual.pdf>,
last accessed date: 11.03.2014
- [9] Yu W, VABS Manual for Users, March 2011,
<http://analyswift.com/wp-content/uploads/2012/10/VABS-Manual.pdf>,
last accessed date: 11.03.2014
- [10] Buhl M L, WT_Perf User's Guide, National Wind Technology Center 2004
- [11] MSC.Nastran 2003 Linear Static User's Guide, MSC Software Corporation, Santa Ana CA USA 2003
- [12] Samcef Wind Turbines (SWT), <http://www.lmsintl.com/simulation/wind-turbines>,
last accessed date: 16/12/2013
- [13] Samcef Mecano, <http://www.lmsintl.com/?sitenavid=8435E5BB-C04D-49AB-B72A-9CB01D6FD9DB>, last accessed date: 02.11.2013
- [14] Samcef Field, <http://www.lmsintl.com/samcef-field>, last accessed date: 30.04.2013